

# Simple Model for the Binding of a Polyelectrolyte to an Oppositely Charged Curved Surface

Gerald S. Manning

Department of Chemistry and Chemical Biology, Rutgers University, 610 Taylor Road, Piscataway, New Jersey 08854-8087

Received: February 18, 2003; In Final Form: August 18, 2003

We present a simple model for the binding of persistence-length segments of a polyelectrolyte to an oppositely charged spherical macroion with radius of the same order as the polymer persistence length. The polyelectrolyte is taken as a rod with elastic bending capacity. The macroion is abstracted as an absolutely rigid circular arc. In the bound state, the polyelectrolyte bends onto the macroion, and some of the opposite charges are mutually neutralized. The curvature of the macroion imposes stability limits on the bound state. The model predicts transitions to bound-state stability in the same conditions (polyelectrolyte charge density and bare persistence length, macroion radius, salt concentration) under which they are observed in experimental studies of the binding of polyelectrolytes to oppositely charged micelles. The calculations also suggest why macroscopic phase separation occurs in experiments below a critical salt concentration but not above.

## 1. Introduction

A series of reports from Paul Dubin's laboratory has documented the transition-like behavior of the binding of polyelectrolytes to oppositely charged spherical macroions such as micelles and dendrimers.<sup>1–5</sup> Similar patterns are observed for binding to globular proteins, and it is assumed that binding occurs in this case to oppositely charged regions of the amphiphilic protein.<sup>5–7</sup> The qualitative experimental trends of the transition points with changes of structural and environmental variables are largely susceptible to explanation in terms of familiar considerations. Thus, the critical surface charge density on the macroion required to bind the polyelectrolyte becomes greater (the polyelectrolyte is harder to bind) at higher salt concentrations, presumably because the electrostatic attraction between macroion and polyion is weakened by the increased salt. Similarly, stiffer polymer chains are harder to bind than more flexible ones, and a given polyion is harder to bind to a smaller macroion than to a larger one, perhaps because it is harder to bend the stiffer chain onto a sphere of given radius or to bend a given chain onto the sphere of smaller radius (larger surface curvature).

Of course, a closer look shows that matters should not be so facilely stated. An important generator of free energy is the chain configurational entropy of the polyelectrolyte that quantifies the many different "crumpled" shapes of roughly equal energy available to the polymer. The loss of some of this entropy when a polymer is adsorbed onto a surface may be one of the decisive components of the free energy, especially if the polymer is long and flexible and the surface is planar or of relatively small curvature.<sup>8</sup> However, if the radius of the sphere chosen to model the macroion is on the same scale as the persistence length of the polymer, then one expects chain entropy to play a diminished role.<sup>9</sup> Direct visual support for neglect of configurational entropy is supplied by the Monte Carlo snapshots of Stoll and Chodanowski, at least for the relatively stiffer polyelectrolytes among those studied.<sup>10</sup>

There must also be a dual role of the electrostatics in these systems. Not only do the opposite charges of macroion and

polyelectrolyte engage in mutual attraction and thus favor complexation, but also charge repulsions within the polyelectrolyte chain disfavor binding by making it harder for the polyelectrolyte to gather itself on the macroion surface. The competing effects of electrostatics can lead in theory to *dissociation* of the complex at low ionic strengths.<sup>9,11,12</sup> A low-salt disruption of the DNA–protein complex called the nucleosome is known,<sup>13</sup> but its structural interpretation is unclear. In that system, the macroion is an octamer of histone proteins, and the DNA is anchored to it along a superhelical ramp of specific sites. There is a possibility that repulsion between adjacent gyres of the DNA superhelix stretches the DNA along the central axis of the superhelix, rupturing the octamer but not releasing the DNA.<sup>14,15</sup>

In the conditions of Dubin's experiments with macroions of stable structure, a low-salt dissociation is not observed (possibly because sufficiently low salt has not yet been looked at).<sup>5</sup> On the other hand, there is an aspect of the data that might be related to intrapolymer electrostatic repulsion. Two polyelectrolytes with equal charge densities but different chain rigidities as measured by their bare persistence lengths were compared.<sup>5</sup> Over most of the salt concentration range studied, the stiffer of the two chains was harder to bind. But as the salt concentration approached about 0.01 M, the binding curves converged. The explanation offered and documented<sup>5</sup> with an analysis of data for the salt dependencies of the persistence lengths was that at lower salt the two chains become equally rigid because the nonspecific electrostatic contribution to chain stiffness is then of greater importance.

Another interesting feature of the experimental data is the phase separation behavior.<sup>5</sup> The bound complex of polyelectrolyte and macroion is soluble at and near the binding threshold. As the binding strength is increased past the threshold, there comes a point at which the complexes either precipitate or coacervate. However, this behavior is observed only below a critical salt concentration. Above the critical level of salt, no macroscopic phase separation occurs. The qualitative explana-

tion may be easier to describe and grasp once we have presented and analyzed our model, so we defer further discussion.

There is a large and often elegant body of theoretical and simulation literature on various aspects of the interaction between polyelectrolytes and oppositely charged curved surfaces.<sup>3,9–12,16–33</sup> It becomes difficult to decide which features of the models are connected to existing experimental data on real systems. We propose here a minimal model for the binding of persistence length segments of a polyelectrolyte to an oppositely charged surface with radius of curvature comparable to the polymer persistence length. The model includes only what is necessary for binding driven by electrostatic attraction against the resistance of the polymer to distortion. A simple formula for the binding free energy is derived. Despite the simplicity of the theory, there is enough in it to predict the existence of binding (wrapping) transitions in realistic experimental conditions. Additionally, partial success is achieved in suggesting why two polymers with different bare persistence lengths nonetheless are observed to converge on the same transition point at low ionic strength (to this end, it helps to augment the model in a crude way to account for intrapolymer charge repulsion). The calculations are consistent with the phase separation behavior of the complexes.

In spirit, our model is perhaps most similar to that of Netz and Joanny<sup>9</sup> and Kunze and Netz.<sup>11,12</sup> Following those authors, we emphasize polymer mechanical stiffness over entropic fluctuations, and we also employ linear (Debye–Hückel) theory, although we use it only in its range of validity. In common with most other authors, Netz et al. model the interaction of the polyelectrolyte and the macroion as a distance-dependent electrostatic attractive potential. This approach is both natural and necessary in the context of their analysis, but our point of view is slightly different. We compare the free energies of a free state and a bound state. We like to think of the bound state as one in which the engaged polyelectrolyte and macroion charges mutually neutralize each other (with surplus charges on one or the other partner in the complex). Thus, we do not introduce an attractive potential. Another difference is our omission (but see below) of the electrostatic repulsions between distant polymer segments that lead Netz et al. to low-salt dissociation of the complex. As mentioned, low-salt dissociation has not been observed in the specific experimental conditions discussed in this paper.

We begin our presentation with a description of the model. Then we proceed to a calculation of its free energy. Numerical examples are provided with parameter values chosen to match experimental conditions, and a discussion tries to connect theory to laboratory data.

## 2. Description of the Model

In experiments, the detection of complex formation is independent of macroion and polymer concentrations and of polymer length.<sup>1–5</sup> Apparently, a tenuous attachment of the polyelectrolyte to the macroion is not recognized. Complexation is observed only when a portion of the polyelectrolyte chain collapses onto the macroion surface. We therefore adopt a two-state model, bound and free. The bound and free states coexist only if their intrinsic free energies are equal, and if they are not equal, the state of lower free energy is stable. A model like this one will automatically exhibit transition-like behavior in experimentally relevant conditions, provided that the free energy difference has a zero at laboratory accessible values of the parameters.

In the free state, there are two noninteracting molecules, the polyelectrolyte A and the macroion B (the polyelectrolyte and

the macroion may be attached at a point, but we do not assign a free energy of interaction to the attachment site). The polyelectrolyte chain is a straight linear lattice of length  $L$ , bearing  $N_A$  charge sites with charge spacing  $b_A = L/N_A$  and reduced charge density  $\xi_A = l/b_A$ , where Bjerrum's length  $l = q^2/(\epsilon kT)$ ,  $q$  is the unit charge,  $\epsilon$  is the dielectric constant of solvent, and  $kT$  is Boltzmann's constant times temperature. The macroion B is a rigid curvilinear lattice of  $N_B$  charge sites with arc length  $L$  (same length as the polyelectrolyte A), charge spacing along the arc  $b_B = L/N_B$ , and corresponding reduced charge density  $\xi_B = l/b_B$ . The curvilinear shape of macroion B is the simplest possible, the arc of a circle, with radius of curvature  $R$ . The charge sites on polyelectrolyte A and macroion B are univalent and of opposite sign. We assume initially that polyelectrolyte A has a higher charge density than macroion B, that is,  $b_A < b_B$ , and  $\xi_A > \xi_B$ . However, this condition will be dropped at the appropriate point of the development.

In the bound state, the rigid macroion B retains its shape as a circular arc of length  $L$  and radius of curvature  $R$ , but the polyelectrolyte A, also of length  $L$ , is wrapped along the macroion arc and therefore has been bent from its initially straight shape to radius of curvature  $R$ . There are fewer charges on the macroion than on the polyelectrolyte, so all of the macroion charges are neutralized by opposite charges on the bound polyelectrolyte. On the other hand, the macroion charges neutralize the fraction  $\alpha$  of the polyelectrolyte charges. If there are originally no charges on the macroion, then  $\alpha$  is zero. When the number of charges on macroion and polyelectrolyte are equal,  $\alpha = 1$ .

As further specification of the model, we assume that the charge density of the polyelectrolyte is below the threshold value for counterion condensation so that Debye–Hückel electrostatics apply. Many experiments and simulations are performed with polymers meeting the condition of subcritical polyelectrolyte charge densities. As far as the macroion is concerned, our initial assumption that its charge density is less than the charge density of the polyelectrolyte automatically places it also below the counterion condensation threshold. When we relax this restriction, we will exercise care that the charge density of the macroion continues to be subcritical.

## 3. Free Energy Calculations

In its free state, polyelectrolyte A has electrostatic free energy  $G_A^{\text{free}}$ ,

$$G_A^{\text{free}} = -N_A kT \xi_A \ln(1 - e^{-\kappa b_A}) \quad (1)$$

where all quantities except  $\kappa$  are as defined in the previous section. The quantity  $\kappa$  is the Debye screening parameter (inverse of the salt screening length).<sup>34,35</sup> If the solvent is aqueous and contains 1:1 salt, then at room temperature a numerical formula for  $\kappa$  in reciprocal nanometers is<sup>34</sup>

$$\kappa = 3.29c^{1/2} \quad (2)$$

where  $c$  is the concentration of the salt in molarity (equal to ionic strength in the 1:1 case). Equation 1 is obtained by summing screened electrostatic potentials from linear Debye–Hückel theory over all pairs of charge sites on the polyelectrolyte.<sup>34</sup> The use of linear theory is justified by the subcritical value of  $\xi_A$ .

In the bound state of polyelectrolyte A, a fraction  $\alpha$  of its charges are neutralized. It therefore carries  $(1 - \alpha)N_A$  charges, its charge density is  $(1 - \alpha)\xi_A$ , and its average charge spacing has increased to  $b_A/(1 - \alpha)$ . Moreover, the polyelectrolyte has

been bent to radius of curvature  $R$ . For the free energy  $G_A^{\text{bound}}$  of polyelectrolyte A in its bound state then, we have

$$G_A^{\text{bound}} = -(1 - \alpha)^2 N_A k T \xi_A \ln(1 - e^{-\kappa b_A/(1-\alpha)}) + \frac{(1 - \alpha)^2 k T \xi_A N_A}{8\kappa^2 R^2} + \frac{L k T \lambda_A}{2R^2} \quad (3)$$

The first two terms on the right-hand side of eq 3 account for electrostatic repulsions among unneutralized charge sites on the polyelectrolyte. They are in fact the first two terms of an expansion in square curvature  $R^{-2}$  of the sum of screened Coulomb potentials among all pairs of unneutralized charges on polyelectrolyte A.<sup>35</sup> For the subcritical value of  $\xi_A$  involved here, the electrostatic term linear in  $R^{-2}$  is identical to the Odijk–Skolnick–Fixman electrostatic bending free energy.<sup>36,37</sup> From its form, it is clear that the linear expansion is adequate only if the radius of curvature  $R$  is larger than the salt screening length  $1/\kappa$ . The third term represents the nonelectrostatic work required to bend polyelectrolyte A from infinite radius of curvature to  $R$ . Thus, it equals the bending free energy of a rod of length  $L$  and elastic bending rigidity  $kT\lambda_A$ , where  $\lambda_A$  is the “bare” polymer persistence length. It does not include the effect of local electrostatic repulsions among the polymer charge sites.

Turning our attention now to macroion B in its free state, we may immediately write (because in its free state rigid macroion B already is curved to radius  $R$ )

$$G_B^{\text{free}} = -N_B k T \xi_B \ln(1 - e^{-\kappa b_B}) + \frac{k T \xi_B N_B}{8\kappa^2 R^2} \quad (4)$$

Finally, macroion B in its bound state has zero free energy because all of its charges are neutralized by charges on polyelectrolyte A (given our running assumption that  $\alpha < 1$ ),

$$G_B^{\text{bound}} = 0 \quad (5)$$

In a next step, we form the free energy difference  $\Delta G = \Delta G_A + \Delta G_B$ , where  $\Delta G_A = G_A^{\text{bound}} - G_A^{\text{free}}$  and  $\Delta G_B = G_B^{\text{bound}} - G_B^{\text{free}}$ . Noting that every term in  $\Delta G$  contains the product  $kT$  as a factor, we find it convenient to regard  $kT$  as our free energy unit, that is, we divide  $\Delta G$  by  $kT$ . It is also useful to consider the free energy per charge site on the free polyelectrolyte. Thus, we make the definition

$$\Delta g = \frac{\Delta G}{N_A k T} \quad (6)$$

When we form the expression for  $\Delta g$ , we encounter the ratio  $N_B/N_A$ , which is equal to  $\alpha$  because all of the charges on macroion B are used to neutralize the fraction  $\alpha$  of charge sites on polyelectrolyte A. Moreover,  $\xi_B = \alpha \xi_A$ , and inversely,  $b_B = b_A/\alpha$ , relations that allow us to eliminate explicit reference to macroion B in our final expression for the free energy. We then have the following formula for  $\Delta g$ , the free energy difference between bound and free states in units of  $kT$  per charge on the polyelectrolyte, where the simpler notations  $b$  and  $\xi$  have replaced  $b_A$  and  $\xi_A$ , respectively:

$$\Delta g = \frac{b\lambda}{2R^2} + \frac{(1 - 2\alpha)\xi}{8\kappa^2 R^2} - (1 - \alpha)^2 \xi \ln(1 - e^{-\kappa b/|1-\alpha|}) + \xi \ln(1 - e^{-\kappa b}) + \alpha^2 \xi \ln(1 - e^{-\kappa b/\alpha}) \quad (7)$$

We now have to explain why in the third term of eq 7 we have written the absolute value of  $1 - \alpha$ , even though to this point

we have assumed that  $\alpha < 1$ , so that  $1 - \alpha$  is automatically positive anyway. The physical meaning of  $\alpha < 1$  is that the macroion has fewer charges than the polyelectrolyte, so the sign of the electrostatic charge on the bound complex is the same as the sign of the charge on the free polyelectrolyte. In other words, the excess charge on the complex comes from the polyelectrolyte. But we can make the opposite assumption that it is the polyelectrolyte that has the fewer charges and the excess charge comes from the macroion. When we go through the calculation again, this time with the latter assumption, which means that  $\alpha > 1$ , we find that  $\Delta g$  comes out to be exactly the same, except that the (positive) term  $\alpha - 1$  appears in the denominator of the exponent instead of  $1 - \alpha$ . Equation 7 as written with the absolute value symbol is therefore applicable to both cases. Note that all terms in  $\Delta g$  are well-behaved at  $\alpha = 1$ , at least mathematically and physically, if not in numerical computer software, which may balk at the single value  $\alpha = 1$ .

We are indebted to a referee for the analysis of the case of excess macroion charge. In a first version of this paper, we had missed this point entirely, and we will see subsequently that it is of great importance in our interpretation of experiments.

#### 4. Numerical Illustrations

Our formula for the free energy difference between bound and free states, eq 7, although resulting from a simple model, contains no fewer than five structural and environmental variables (not counting temperature and solvent dielectric constant), namely, the polyelectrolyte charge spacing  $b$  and its correlated charge density  $\xi$ , the radius  $R$  of the macroion, the degree of neutralization  $\alpha$ , the bare (nonelectrostatic) persistence length  $\lambda$  of the polyelectrolyte, and the salt concentration  $c$  implicit in the Debye length  $1/\kappa$ . Our hope is that the model will exhibit binding transitions when experimentally relevant values are given to these parameters.

In the experiments of Kayitmazer et al.,<sup>5</sup> both polyelectrolyte species studied have equal charge densities,  $\xi = 0.56$ , and the micelle to which the polyelectrolyte binds has radius  $R = 2$  nm. In the following numerical illustrations, we therefore fix  $\xi$  and  $R$  at these values. Note that the polyelectrolyte charge density is less than unity, the threshold value for counterion condensation for univalent counterions. Our Debye–Hückel equations also require that the charge density of the macroion be less than unity, so the range of  $\alpha$  values must cut off at about 1.8, where  $\xi_B = (1.8)(0.56) = 1$ . The lowest salt concentration used by Kayitmazer et al. is 0.01 M, corresponding to Debye screening length about 3 nm, which means that in the worst case,  $\kappa R$  is about  $2/3$ , while for strict validity of our approximation for the electrostatic contribution to bending, this product should exceed unity. We will cut off our theoretical curves at  $c = 0.01$  M. We will see that the electrostatic contribution to bending is not a large contribution anyway.

We look at the effects of varying the extent of neutralization  $\alpha$ , the salt concentration  $c$ , and the bare persistence length  $\lambda$ . The two polyelectrolytes used by Kayitmazer et al. have bare persistence lengths equal to 2.95 and 4 nm, respectively, and we use these values. Figures 1–3 illustrate the transition from free to bound state upon variation in turn of one variable from the set  $(\alpha, c, \lambda)$ , keeping the others fixed. The crossover from positive to negative values of  $\Delta g$  signifies the onset of stability of the bound state. From Figure 1, we see that the bound state emerges when the extent of charge neutralization increases past a critical value. In Figure 2, the bound state appears when the salt concentration decreases below a critical value. Finally, Figure 3 shows that a relatively flexible polyelectrolyte can be

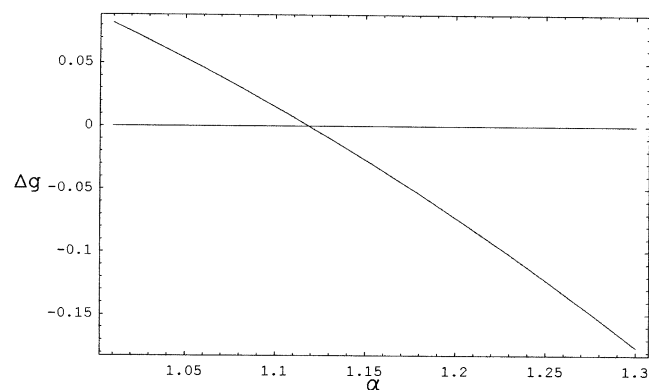


**Figure 1.** A plot of the binding free energy as a function of the fractional extent of neutralization of the polyelectrolyte. The negative values for  $\alpha > 1.12$  indicate the range of stability of the bound state for the following parameter values: polyelectrolyte charge spacing  $b = 1.25$  nm ( $\xi = 0.56$ ); bare persistence length of polyelectrolyte  $\lambda = 2.95$  nm; radius of curvature of macroion  $R = 2$  nm; salt concentration  $c = 0.1$  M.

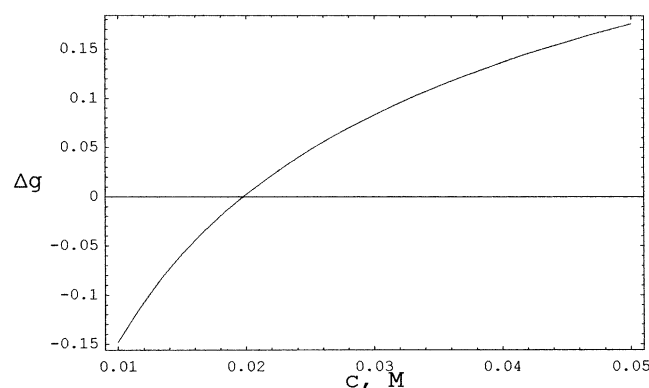


**Figure 2.** A plot of binding free energy as a function of salt concentration. The negative values for  $c < 0.020$  M indicate the range of stability of the bound state for the parameter values  $b = 1.25$  nm ( $\xi = 0.56$ ),  $\lambda = 2.95$  nm,  $R = 2$  nm, and  $\alpha = 0.5$ .

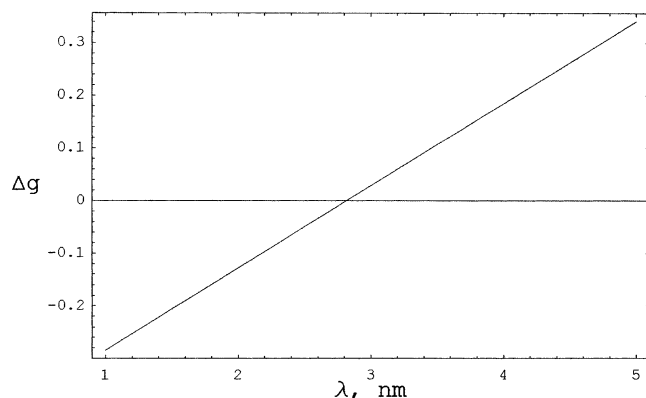


**Figure 3.** A plot of binding free energy as a function of bare persistence length. The negative values for  $\lambda < 2.82$  nm indicate the range of stability of the bound state for the parameter values  $b = 1.25$  nm ( $\xi = 0.56$ ),  $R = 2$  nm,  $\alpha = 0.8$ , and  $c = 0.05$  M.

bound, while a stiffer one of the same charge density and in the same conditions does not bind. In all three figures, the transition occurs at values of salt concentration and persistence length relevant to experiment.<sup>5</sup> The values of  $\alpha$  involved are physically reasonable, indicating comparable charge densities of macroion and polyelectrolyte.

Figure 1 shows  $\Delta g$  as a function of  $\alpha$  for a fixed ionic strength  $c = 0.1$  M. The crossover to stability of the bound state occurs at the critical value  $\alpha_{\text{crit}} = 1.12$ , where  $\Delta g = 0$ . For different

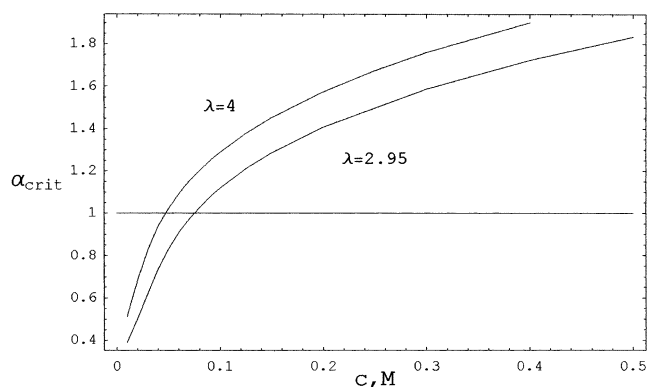


**Figure 4.** The dependence of the critical extent of neutralization on salt concentration for two values of bare persistence length (nm). For each curve,  $b = 1.25$  nm ( $\xi = 0.56$ ) and  $R = 2$  nm.

values of  $c$ , the root  $\alpha_{\text{crit}}$  of the equation  $\Delta g = 0$  takes different values. In Figure 4, we present plots of  $\alpha_{\text{crit}}$  vs  $c$  for two different values of the bare persistence length  $\lambda$ , and we discuss the motivation from experiments for this representation and its various aspects in the next section. The value  $\alpha_{\text{crit}} = 1$  has been marked out in Figure 4 for reasons to be discussed.

## 5. Discussion

A striking aspect of the experiments involving binding of a polyelectrolyte to an oppositely charged macroion is the transition-like behavior observed.<sup>1–7</sup> Binding occurs only on crossing threshold values of the probe variables such as the surface charge density of the macroion, pH, salt concentration, and so forth. Figures 1–3 show that the model considered here contains this important general feature for values of the model parameters that are relevant to real experimental conditions. In the model, it is the finite radius of curvature  $R$  of the macroion that causes the appearance of critical conditions for stability of the bound state. If in eq 7 we take  $R$  equal to infinity, then the first two terms on the right-hand side are annulled and the resulting  $\Delta g$  is the free energy difference between bound and free states of a rodlike polyelectrolyte and a rigid “macroion” that lacks curvature (analogue of a planar surface). This  $\Delta g$  is always negative, so in the absence of forced polyelectrolyte bending, the bound state is always stable (this conclusion is valid only in the framework of a rodlike model for the polyelectrolyte).<sup>8</sup>

One way of doing an experiment in this field is to increase the surface charge density of the macroion until binding of the oppositely charged polyelectrolyte is detected.<sup>1–5</sup> The critical surface charge density is then reported. In our model, the macroion surface charge density is represented by the curvilinear charge density  $\xi_B$  of our circular-arc model for the macroion. The free energy of binding  $\Delta g$  is positive at  $\alpha = 0$  (the bound state is not stable in the absence of any charge neutralization). As  $\alpha$  increases from zero but remains less than one, all of the charge on the macroion is used to neutralize the fraction  $\alpha$  of the charges on the polyelectrolyte ( $\alpha = \xi_B/\xi_A < 1$ ). If in this range, a minimum value  $\alpha_{\text{crit}}$  is encountered where  $\Delta g = 0$ , then a transition to stability of the bound state occurs. This critical value of  $\alpha$  is plotted in Figure 4 as a function of salt concentration for two polyelectrolytes of different persistence lengths but equal charge densities. On the contrary, it may happen that  $\Delta g$  remains positive all the way up to  $\alpha = 1$ ; not enough charge has been placed on the macroion to bind the polyelectrolyte even though the macroion is capable of neutralizing 100% of the polyelectrolyte charge. The polyelectrolyte



is too stiff. We can continue to charge up the macroion past this point. Now  $\alpha$  becomes greater than one. The charge on the macroion exceeds the charge on the polyelectrolyte ( $\alpha = \xi_B/\xi_A > 1$ ). In the range  $\alpha > 1$ , there does then come a minimum value  $\alpha_{\text{crit}}$  where  $\Delta g = 0$  and a transition to bound state stability occurs. Figure 4 includes this range of critical values of  $\alpha$  as well, but we have imposed a cutoff at  $\alpha = 1.8$ , which marks the end of the domain of validity of the Debye–Hückel approximation for our model of the free macroion.

We are unable to make a quantitative comparison of the theoretical plots in Figure 4 with the data of Kayitmazer et al.<sup>5</sup> because in the experiments it is the surface charge density of a spherical micelle that is varied, while we vary the linear charge density of a circular arc that is supposed to represent the micelle. However, we can discuss certain aspects of Figure 4 that suggest some relation to the experimental data. In this qualitative discussion, we think of  $\alpha_{\text{crit}}$  as synonymous with the surface charge density on the micelle. First of all, the critical macroion charge density is seen to increase with salt concentration across the entire range. The polyelectrolyte is harder to bind at higher salt, in agreement with the data. Second, the range of salt concentrations shown, 0.01–0.5 M, is the same as the range used in the experiments. Combined with our use of the same values of persistence length and macroion radius that characterized the materials in the experiments, this observation shows that the model predicts the transition to a stable complex in the same conditions under which the transitions are found in the laboratory. Third, in accord with measurement, the stiffer polyelectrolyte is harder to bind (its curve lies above the curve for the more flexible chain).

Aside from the obvious trends in Figure 4, there are two more subtle features that are nonetheless of interest. Although the stiffer polyelectrolyte is harder to bind—everywhere in Figure 4 and over most of the salt range in the experiments—the experimental data converge completely at low salt (0.01 M), so the bare persistence length must not be what determines the resistance of the polyelectrolyte to binding at low salt. Kayitmazer et al. propose that the resistance to binding comes from the total persistence length of the polyelectrolyte, which includes electrostatic stiffening. They further suggest that the electrostatic contribution, which is presumably independent of the bare persistence length, becomes dominant at low salt, and they support their proposal with data on the ionic strength dependence of total persistence length for the two polymers that they have used.

In Figure 4, we see a hint of convergence at low salt; the spread between the two curves at 0.01 M is 70% of the spread at 0.1 M. The contribution to  $\Delta g$  that comes from the polyelectrolyte's resistance to bending is given by the expression (see eq 3)

$$\frac{b\lambda}{2R^2} + \frac{(1-\alpha)^2\xi}{8\kappa^2R^2} \quad (8)$$

where the second term represents the electrostatic stiffening. The electrostatic term does become of enhanced significance at lower salt. At 0.1 M salt, it can be checked that it is virtually negligible. At 0.01 M, it is about 9% of the combined two terms. In our model, this term does not dominate the bending resistance at the lowest salt concentration considered, and the tendency toward convergence in Figure 4 is far from complete. Convergence is in fact completed at 0.0001 M salt, but we have not extended Figure 4 down this far because the expression that we have used for the electrostatic stiffening would then be far

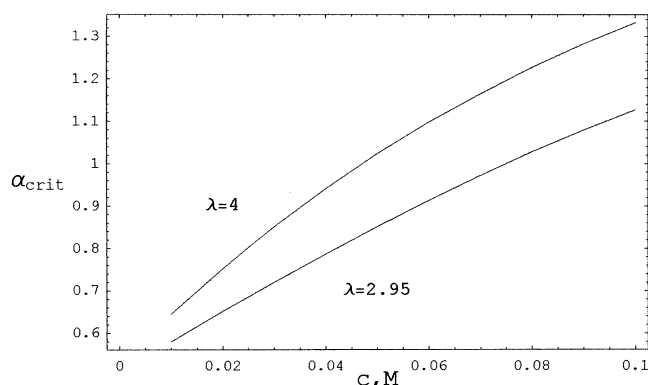


**Figure 5.** The dependence of the critical extent of neutralization on salt concentration for two values of bare persistence length (nm) with inclusion of distant intrapolymer repulsion as described in the text. For each curve,  $b = 1.25$  nm ( $\xi = 0.56$ ) and  $R = 2$  nm.

outside its range of validity and, besides, the experiments indicate that convergence is achieved at 0.01 M.

Our expression for  $\Delta g$  in eq 7 contains no contribution from possible electrostatic repulsion between polyelectrolyte segments collapsed on the macroion. Within the confines of our model, it is not possible to make a rigorous accounting of this effect. As an ad hoc device, however, we may add to  $\Delta g$  the term

$$2(1-\alpha)^2\xi K_0(\kappa d) \quad (9)$$

where the last factor is a Bessel  $K$ -function (modified Bessel function of the second kind of order zero). This expression is the Debye–Hückel free energy needed to bring two lines of charge from infinity into parallel orientation with separation distance  $d$ . It crudely estimates the effect of electrostatic crowding among polymer segments distant along the chain when the segments are forced to gather themselves near the macroion surface. For  $d$ , we might take the value 1 nm as a reasonable guess at an effective distance of closest approach of two polyelectrolyte segments. With  $\Delta g$  thus augmented, we have constructed Figure 5 for the lower end of the salt range, and here we see a stronger tendency toward convergence, the spread between the two curves at 0.01 M being only a third of the spread at 0.1 M.

All in all, our model is consistent with an interpretation of the experimental data that for most of the salt range attributes resistance to complex formation primarily to the mechanical bending resistance of the polymer (bare persistence length); while at low salt, the electrostatic intrapolymer repulsion becomes dominant, manifesting itself as some combination of local electrostatic stiffening (electrostatic persistence length) and repulsion among the polyelectrolyte segments gathered on the surface of the macroion.

We have mentioned the presence of a second subtle feature in Figure 4, and in its connection, we have singled out the value  $\alpha_{\text{crit}} = 1$ . Each curve in Figure 4 passes smoothly through this value, and there is no mathematical reason for distinguishing the two branches  $\alpha_{\text{crit}} < 1$  and  $\alpha_{\text{crit}} > 1$ . But there is a physical reason. In our model, when  $\alpha_{\text{crit}} < 1$ , all of the charges on the macroion are neutralized and the complex bears the excess charge of the polyelectrolyte. When  $\alpha_{\text{crit}} > 1$ , all of the charges on the polyelectrolyte are neutralized and the complex bears the excess charge of the macroion. At  $\alpha_{\text{crit}} = 1$ , the complex is isoelectric. Motivated by the discussion below, we define a critical salt concentration,  $c^*$ , as the salt concentration for which  $\alpha_{\text{crit}} = 1$ . For each curve in Figure 4,  $c^*$  is the value of  $c$  at which the horizontal line cuts the curve. For the stiffer

polyelectrolyte,  $c^* = 0.047$  M, and for the more flexible one,  $c^* = 0.074$  M.

Kayitmazer et al. have discovered a critical  $c^*$  in their experiments.<sup>5</sup> They have noticed that there is an apparent difference in the nature of the complex that forms at a salt concentration less than  $c^*$  compared to the complexes formed in salt of concentration greater than  $c^*$ . The low-salt complexes ultimately aggregate, and macroscopic phase separation is observed when the charge density on the micelle is increased (at fixed low salt) beyond its threshold value for incipient soluble complex formation. No macroscopic phase separation is observed for the complexes formed at high salt.

The interpretation offered by Kayitmazer et al. for their observations concerning phase separation is as follows. Macroscopic phase separation occurs if a sufficient number of charge neutral complexes are present. The threshold value of micelle surface charge density required for incipient formation of soluble complex is low if the complex is formed at low salt. The complex is soluble because it bears an excess charge (of sign determined by the polyelectrolyte). The complexes that form in increasing numbers from micelles of progressively higher postthreshold surface charges (at the same fixed low salt concentration) approach a charge neutral state. Macroscopic phase separation occurs when the complex becomes charge neutral. A different behavior is exhibited by soluble complexes incipiently formed at high salt because the stability of the complex then requires that the threshold charge on the micelle be high. The complex bears an excess charge of sign determined by the micelle. Further increases of charge on the micelle (at the same fixed high salt concentration) can only increase the excess charge of the complex. The complex never attains a charge neutral state, and therefore, phase separation is not observed.

If we compare the interpretation of Kayitmazer et al. of their observations concerning phase separation with our discussion of the two branches of the plots in Figure 4, we see that our model is suited to the interpretation. The low-salt and high-salt complexes in terms of our model can be identified as those formed at  $\alpha_{\text{crit}} < 1$  and  $\alpha_{\text{crit}} > 1$ , respectively. The two branches of the model occur in the same range of salt concentrations at which Kayitmazer et al. see a change in the nature of the soluble complex.

It would be nice if the values of  $c^*$  observed by Kayitmazer et al. were in quantitative agreement with the values that arise in our model. They are not. In our model,  $c^* = 0.047$  M for the stiffer polyelectrolyte, while the value reported by Kayitmazer et al. (for a real polyelectrolyte with the same bare persistence length and charge density as our stiffer polyelectrolyte) is 0.100 M. For the more flexible polyelectrolyte, the corresponding values are 0.074 M (theory) and 0.175 M (experiment). The theoretical values in both cases are about a

factor of 2 lower than the measured ones. Both theory and experiment agree that the value of  $c^*$  is lower for the stiffer polyelectrolyte.

**Acknowledgment.** The author thanks Paul Dubin, Basak Kayitmazer, and Roland Netz for valuable correspondence. As mentioned in the text, he is indebted to the referee for pointing out the necessity of extending the  $\alpha$  range to values greater than unity.

## References and Notes

- (1) Dubin, P. L.; Thé, S. S.; McQuigg, D. W.; Chew, C. H.; Gan, L. M. *Langmuir* **1989**, *5*, 89.
- (2) Feng, X. H.; Dubin, P. L.; Zhang, H.; Kirton, G. F.; Bahadur, P.; Parotte, J. *Macromolecules* **2001**, *34*, 6373.
- (3) Zhang, H.; Dubin, P. L.; Ray, J.; Manning, G. S.; Moorefield, C. N.; Newkome, G. R. *J. Phys. Chem. B* **1999**, *103*, 2347.
- (4) Miura, N.; Dubin, P. L.; Moorefield, C. N.; Newkome, G. R. *Langmuir* **1999**, *15*, 4245.
- (5) Kayitmazer, A. B.; Seyrek, E.; Dubin, P. L.; Staggemeier, B. A. *J. Phys. Chem. B*, in press.
- (6) Xia, J.; Dubin, P. L.; Kim, Y.; Muhoherac, B. B.; Klimkowski, V. *J. J. Phys. Chem.* **1993**, *97*, 4528.
- (7) Mattison, K. W.; Dubin, P. L.; Brittain, I. J. *J. Phys. Chem. B* **1998**, *102*, 3830.
- (8) Netz, R. R.; Andelman, D. *Phys. Rep.*, in press. arXiv:cond-mat/0203364 v2 12 Feb 2003.
- (9) Netz, R. R.; Joanny, J.-F. *Macromolecules* **1999**, *32*, 9026.
- (10) Stoll, S.; Chodanowski, P. *Macromolecules* **2002**, *35*, 9556.
- (11) Kunze, K. K.; Netz, R. R. *Phys. Rev. Lett.* **2000**, *85*, 4389.
- (12) Kunze, K. K.; Netz, R. R. *Phys. Rev. E* **2002**, *66*, 011918.
- (13) van Holde, K. E. *Chromatin*; Springer-Verlag: New York, 1989.
- (14) Marky, N. L.; Manning, G. S. *Biopolymers* **1991**, *31*, 1543.
- (15) Gavin, I. M.; Usachenko, S. I.; Bavykin, S. G. *J. Biol. Chem.* **1998**, *273*, 2429.
- (16) Weigel, F. W. *J. Phys. A: Math. Gen.* **1977**, *10*, 299.
- (17) Odijk, T. *Macromolecules* **1980**, *13*, 1542.
- (18) Evers, O. A.; Fleer, G. J.; Scheutjens, J. M. H. M.; Lyklema, J. *Colloid Interface Sci.* **1986**, *111*, 446.
- (19) von Goeler, F.; Muthukumar, M. J. *Chem. Phys.* **1994**, *100*, 7796.
- (20) Kong, C. Y.; Muthukumar, M. J. *Chem. Phys.* **1998**, *109*, 1522.
- (21) Marky, N. L.; Manning, G. S. *J. Mol. Biol.* **1995**, *254*, 50.
- (22) Mateescu, E. M.; Jeppesen, C.; Pincus, P. *Europhys. Lett.* **1999**, *46*, 493.
- (23) Park, S. Y.; Bruinsma, R. F.; Gelbart, W. M. *Europhys. Lett.* **1999**, *46*, 454.
- (24) Gurovitch, E.; Sens, P. *Phys. Rev. Lett.* **1999**, *82*, 339.
- (25) Schiessel, H.; Rudnick, J.; Bruinsma, R.; Gelbart, W. M. *Europhys. Lett.* **2000**, *51*, 237.
- (26) Schiessel, H.; Bruinsma, R. F.; Gelbart, W. M. *J. Chem. Phys.* **2001**, *115*, 7245.
- (27) Nguyen, T. T.; Shklovskii, B. I. *Physica A* **2001**, *293*, 324.
- (28) Haronska, P.; Vilgis, T. A.; Grottenmüller, R.; Schmidt, M. *Macromol. Theory Simul.* **1998**, *7*, 241.
- (29) Wallin, T.; Linse, P. *J. Phys. Chem. B* **1997**, *101*, 5506.
- (30) Jonsson, M.; Linse, P. *J. Chem. Phys.* **2001**, *115*, 10975.
- (31) Akinchina, A.; Linse, P. *Macromolecules* **2002**, *35*, 5183.
- (32) Chodanowsky, P.; Stoll, S. *J. Chem. Phys.* **2001**, *115*, 4951.
- (33) Chodanowsky, P.; Stoll, S. *Macromolecules* **2001**, *34*, 2320.
- (34) Manning, G. S. *Q. Rev. Biophys.* **1978**, *11*, 179.
- (35) Manning, G. S. *Macromolecules* **2001**, *34*, 4650.
- (36) Odijk, T. *J. Polym. Sci.* **1977**, *15*, 477.
- (37) Skolnick, J.; Fixman, M. *Macromolecules* **1977**, *10*, 944.